High-order discrete fourier transform for the solution of the Poisson equation

Federica Caforio, Sébastien Imperiale

HIGH-ORDER DISCRETE FOURIER TRANSFORM FOR THE SOLUTION OF THE POISSON EQUATION *

F. CAFORIO † AND S. IMPERIALE ‡

Abstract. The aim of this work is to propose a novel, fast, matrix-free solver for the Poisson problem discretised with High-Order Spectral Element Methods (HO-SEM). This method is based on the use of the Discrete Fourier Transform to reduce the problem to the inversion of the symbol of the operator in frequency space. The solver proposed is endowed with several properties. First, it preserves the efficiency of standard FFT algorithm; then, the matrix storage is minimised; a pseudo-explicit Singular Value Decomposition (SVD) is used for the inversion of the symbols; finally, it can be easily extended to multiple dimensions and non-periodic boundary conditions. In particular, due to the underlying HO-SEM discretisation, the multi-dimensional symbol of the operator can be efficiently computed from the one-dimensional symbol by tensorisation.

Key word. Fast Fourier transform, high-order finite elements, Poisson's equation

AMS subject classifications. 65T99, 65N30

1. Introduction.

The objective of this work is to provide a fast method to solve the Poisson partial differential equation (PDE) in bounded domains. This topic has already been largely addressed in the literature (see [17, 11] or more recently [14, 3]). However, to our best knowledge, there is no efficient algorithm that is adequate for the specific applications we target. In more detail, we require a fast method that is compatible (in a sense that will be specified in what follows) with high-order Finite Element (FE) discretisations. The main application is the treatment of the incompressibility condition for transient elastodynamic or Navier-Stokes PDEs (see [10]). In these PDEs, although parameters may be heterogeneous and/or anisotropic, the treatment of the incompressibility constraint is reduced to the solution of a Poisson equation for a scalar unknown, i.e. the pressure, thanks to penalisation techniques.
Advanced methods involve the solution of these PDEs (Stokes or elastodynamics) with high-order FE methods, and it can be shown that the pressure must be solved in an suitable High-Order (HO) FE space, in order to satisfy a stability condition, namely a discrete inf-sup condition (we refer to [6, 5] for further details).
A well-known FE method for Stokes flow and transient elastodynamics problems is the so-called Spectral Element Method (SEM) (see [15] for Stokes equation, [13] for seismic wave equations and [9] for elastodynamics). Two main assets of this type of FE methods are the optimal rate of convergence achieved and mass-lumping. Therefore, they represent a privileged choice for explicit discretisation of transient problems. Furthermore, they are constructed in one-dimension from Lagrangian basis functions supported on Gauss-Lobatto points, and their extension to two- and three-dimensions is straightforward, since it is based on tensorisation.
Due to the aforementioned inf-sup condition, the choice of space discretisation for the main unknown restricts the choice for the auxiliary variable, i.e. the pressure. In more detail, it is shown in [5] that if $(R+1)$-order continuous SEM are used for the main unknown, and a regular rectangular mesh is considered, it is possible to use R continuous SEM for the pressure, still keeping the optimal order of convergence, and

*Submitted to the editors November 6, 2018.

†federica.caforio@inria.fr. Inria, Université Paris-Saclay, France. LMS, Ecole Polytechnique, CNRS, Université Paris-Saclay, France.

‡sebastien.imperiale@inria.fr. Inria, Université Paris-Saclay, France. LMS, Ecole Polytechnique, CNRS, Université Paris-Saclay, France.

the inf-sup constant does not depend on the size of the mesh. Note, however, that [2] have provided numerical evidence that the inf-sup constant decays as the order of polynomials increases.
In this paper we construct a fast, matrix-free solver for the Poisson problem discretised with HO-SEM on uniform meshes. The main peculiarity of this method is that it corresponds to the explicit computation of the inverse of the discrete Laplace operator (computed with HO-SEM), hence accuracy and convergence properties of the solver are directly inherited from those of the SEM.
The proposed method relies on the use of the Fast Fourier Transform (FFT), to reduce the problem in the inversion of the – frequency-dependent – symbol of the operator. When first-order finite elements are adopted, the symbol is scalar, its inversion is trivial and the solution is recovered using inverse FFT (this is the classical fast method presented in many textbooks, see for instance [11, 12]). When high-order FE are used, the symbol is no-longer scalar, and its inversion is no longer trivial. The definition of this symbol has been first introduced in ([8, 1]) for the discrete analysis of wave propagation phenomena in periodic domains but, surprisingly, it has never been used as an actual solver for the Poisson equation. The solver we construct has the following algorithmic properties: first, it preserves the efficiency of standard FFT algorithm; then, it minimises matrix storage; a pseudo-explicit Singular Value Decomposition (SVD) is used for inversion of the symbols; finally, it is extended to the treatment of Neumann and Dirichlet boundary conditions.
This paper is organised as follows. Section 2.1 contains the main features of the Poisson-like partial differential equation that we aim to solve and its numerical approximation by standard Spectral Element Methods. Then, in Section 2.2 we recall the standard method based on FFT. In Section 3 an efficient method for the solution of the problem with high-order space approximation and periodic boundary conditions (BCs) is described. This method is derived as a generalisation of the standard FFT algorithm. This section also contains further details on the practical implementation of the method. Sections 3.2 and 4 are devoted to the generalisation to other BCs, e.g. Dirichlet and Neumann, and the extension to multiple dimensions, respectively. Numerical results are shown in Section 5, along with some remarks on the complexity of the solver – which is shown to be in $O(R^{d+1}\,N^d\,\log N)$ in dimension d on meshes with N^d elements – and its parallelisability.

2. Statement of the problem and standard results.

2.1. Variational formulation for the Poisson problem. Let us consider a generalisation of the Poisson equation in $\Omega \subset \mathbb{R}^d$: $\rho\, u - \Delta u = f$, with u and f scalar functions, and $\rho \in \mathbb{C}$ is a constant with non zero imaginary part or with non negative real part. We do not specify the conditions imposed on the boundary of Ω for the moment. Given an admissible subspace $\mathcal{V} \subset H^1(\Omega)$, we want to solve the following related variational formulation : *Find* $u \in \mathcal{V}$ *such that*

$$\rho\, m(u,v) + a(u,v) = \ell(v), \quad \forall v \in \mathcal{V}, \tag{2.1}$$

where

$$m(u,v) = \int_\Omega u\,\overline{v}\,\mathrm{d}\Omega, \quad a(u,v) = \int_\Omega \underline{\nabla} u \cdot \overline{\underline{\nabla} v}\,\mathrm{d}\Omega, \quad \ell(v) = \int_\Omega f\,\overline{v}\,\mathrm{d}\Omega.$$

For the space discretisation, we introduce a finite-dimensional subspace $\mathcal{V}_h \subset \mathcal{V}$ of continuous functions. The discrete problem reads: *Find* $u_h \in \mathcal{V}_h$ *such that*

$$\rho\, m_h(u_h, v_h) + a_h(u_h, v_h) = \ell_h(v_h), \quad \forall\, v_h \in \mathcal{V}_h, \tag{2.2}$$

where

$$m_h(u_h, v_h) = \int_\Omega^Q u_h\, \overline{v_h}\, \mathrm{d}\Omega, \quad a_h(u_h, v_h) = \int_\Omega^Q \underline{\nabla} u_h \cdot \overline{\underline{\nabla} v_h}\, \mathrm{d}\Omega,$$

and we assume that there exists $f_h \in \mathcal{V}_h$ such that $\ell_h(v_h) = m_h(f_h, v_h)$. Note that the superscript Q on the integral signs denotes approximation by quadrature rule. We recall that in one-dimension, given a function f, an $(R_Q+1)-$points quadrature rule is based on a suitable set of points $\{\eta_k\}$ in $[0,1]$ and weights $\{\omega_k\}$ such that

$$\int_{[0,h]} f(x)\, \mathrm{d}x \approx \int_{[0,h]}^Q f(x)\, \mathrm{d}x \coloneqq h \sum_{k=0}^{R_Q} f(\eta_k\, h)\, \omega_k. \tag{2.3}$$

We recall that if Gauss-Lobatto nodes are used, this formula is exact for polynomials up to degree $2R_Q - 1$ (see for instance [16] for more details). Fast methods can be used solve (2.2) , see for example the hierarchical matrix (H-matrix) method ([4]), that is an efficient algorithm to compute approximate inverse matrices based on data-sparse approximations of non-sparse matrices. Within this family of methods, the most efficient one relies on the use of the Fast Fourier Transform (FFT). The use of this method is, however, restricted to some assumptions on the computational domain – Ω is a rectangle in 2-D, or a parallelepiped in 3-D – and to the use of $\mathcal{Q}^1$ finite elements for constructing $\mathcal{V}_h$ (see for example [11, 12]). The next section is devoted to a recap of this solver (in one-dimension). The solver we propose in this article represents a generalisation of the aforementioned algorithm for high-order discretisation.

2.2. A fast solver based on FFT in one-dimension. The briefly recall the standard Fast Fourier Transform (FFT), let us consider the one-dimensional case. We assume that the computational domain is $[0, L]$. If ones uses $\mathcal{P}^1$ Lagrange shape functions, we have

$$u_h(x) = \sum_{j=0}^{N} u_j \varphi_j(x), \quad v_h(x) = \sum_{j=0}^{N} v_j \varphi_j(x), \quad f_h(x) = \sum_{j=0}^{N} f_j \varphi_j(x) \tag{2.4}$$

as well as periodic boundary condition, i.e. $u_N \equiv u_0$. We assume that the source term f_h is continuous and L-periodic (i.e. it belongs to $C^0_\sharp([0, L])$) and its values $f_n \coloneqq f_h(x_n)$ are given at the grid points

$$x_n = n\, h, \quad n \in \mathcal{N}, \quad N\, h = L,$$

where we have defined $\mathcal{N} = \{0, 1, .., N-1\}$. Based on these known values, we can construct an interpolation function

$$\tilde{f}_h(x) = \frac{1}{N} \sum_{k \in \mathcal{N}} \hat{f}_k\, e^{\frac{i 2\pi x k}{N}}, \tag{2.5}$$

that should agree with f_h at the grid points. This is guaranteed by the use of the Discrete Fourier Transform (DFT) of the function f_h and its inverse, called Inverse Discrete Fourier Transform (IDFT). It is possible to prove the proposition ([11]) below.

PROPOSITION 2.1. *Let $f_h \in C^0_\sharp([0,L])$ and $\tilde{f}_h \in C^0_\sharp([0,L])$ be defined by (2.5). Then,*

$$f_h(x_n) = \tilde{f}_h(x_n),\ \forall n \in \mathcal{N} \iff \hat{f}_k = \sum_{n\in\mathcal{N}} f_h(x_n)\, e^{-\frac{ik2\pi nh}{L}},\ \forall k \in \mathcal{N}$$
$$\iff f_h(x_n) = \frac{1}{N}\sum_{k\in\mathcal{N}} \hat{f}_k\, e^{\frac{ik2\pi nh}{L}},\ \forall n \in \mathcal{N}.$$

The basic ingredient to prove this proposition is the following orthogonality property:

$$\sum_{\ell\in\mathcal{N}} e^{-\frac{i\ell 2\pi nh}{L}}\, e^{-\frac{ik2\pi nh}{L}} = \delta_{k,\ell}, \quad \forall k,n \in \mathcal{N}. \tag{2.6}$$

Derivation of the symbol of the operator. If we adopt for the computation of each integral the midpoint rule, on an interval $[a,b],\ a<b$,

$$\int_{[a,b]}^{Q} g(x)dx = \frac{b-a}{2}\big(g(0)+g(1)\big),$$

then we end up with the finite-difference scheme (with the convention $u_{-1} = u_{N-1}$)

$$\rho\, u_n\, h - \frac{1}{h}\Big(u_{n+1} + u_{n-1} - 2\,u_n\Big) = f_n\, h \quad n \in \mathcal{N}. \tag{2.7}$$

Analogously, we can construct an interpolation function for the solution $u_h(x)$, that reads

$$\tilde{u}_h(x) = \frac{1}{N}\sum_{k\in\mathcal{N}} \hat{u}_k\, e^{\frac{i2\pi xk}{N}} \quad \text{and} \quad \hat{u}_k = \sum_{n\in\mathcal{N}} u_n\, e^{-\frac{ik2\pi nh}{L}},\ \forall n \in \mathcal{N}, \tag{2.8}$$

and, therefore, thanks to Proposition 2.1, $\tilde{u}_n \coloneqq \tilde{u}(x_n) = u_n$, for all $n \in \mathcal{N}$. Denoting again, $\tilde{u}_{-1} = \tilde{u}_{N-1}$, we obtain that

$$\rho\, \tilde{u}_n\, h - \frac{1}{h}\Big(\tilde{u}_{n+1} + \tilde{u}_{n-1} - 2\,\tilde{u}_n\Big) = \tilde{f}_n\, h \quad n \in \mathcal{N}. \tag{2.9}$$

By definition of the interpolation functions in Eqs. (2.5) and (2.8) and due to the orthogonality property (2.6), we get the following equations

$$\mathcal{S}_k \hat{u}_k = \hat{f}_k, \quad \mathcal{S}_k \coloneqq \Big(\rho - \frac{2}{h^2}(\cos(2\pi kh/L) - 1)\Big),\ \forall k \in \mathcal{N}, \tag{2.10}$$

where $\mathcal{S}_k$ is called the symbol of the operator associated with Eq. (2.7).

The algorithm. The complete algorithm for the solution of Problem (2.7) can be deduced from (2.10) and can be resumed in three main steps:

1. Perform a DFT of the discrete source term for each element

$$\hat{f}_k = \sum_{n\in\mathcal{N}} f_n\, e^{-\frac{ik2\pi nh}{L}},\ \forall k \in \mathcal{N};$$

2. Apply the inverse symbol of the operator

$$\hat{u}_k = \mathcal{S}_k^{-1}\hat{f}_k, \quad k \in \mathcal{N};$$

3. Perform an inverse DFT of the solution for each frequency

$$u_n = \frac{1}{N} \sum_{k \in \mathcal{N}} \hat{u}_k \, e^{\frac{ik2\pi nh}{L}}, \ \forall n \in \mathcal{N}.$$

This algorithm has several advantages. First, no storage of finite element matrices is required (as for any finite difference schemes). Furthermore, the problem for each frequency k is decoupled. Therefore, operations at each step can be performed in parallel on the frequencies. At last, the first and third steps can be performed by Fast Fourier Transform (FFT) algorithm. This algorithm is efficient: the computation of a FFT of N points requires $O(N \log N)$ arithmetical operations.

3. The High-Order Spectral Element FFT solver in one-dimension.

3.1. Periodic boundary conditions. If higher-order approximation in space is considered for the numerical solution of Eq. (2.2), the Fourier-based method described above is not suitable and needs to be generalised. First, we introduce the framework for higher-order spatial approximation of Eq. (2.2). This formulation is inspired by [1] and [7]. For the sake of clarity, we consider a one-dimensional domain of size $[0, L]$ and impose periodic boundary conditions (BCs) at first. We refer the reader to Sections 3.2 and 4 for the extension to Neumann and Dirichlet BCs and to multiple dimensions, respectively.

Let $\mathcal{V}_{h,R}$ be the approximation space for continuous piecewise R-order polynomials in $[0, L]$. We introduce a basis of shape functions $\left\{\varphi_{n,j}\right\}_{n\in\mathcal{N},\, j\in\mathcal{R}}$ with $\mathcal{N} = \{0, 1, .., N-1\}$, $\mathcal{R} = \{0, 1, .., R-1\}$, such that

$$\text{Supp}(\varphi_{n,0}) = [(n-1)h, (n+1)h], \forall n \in \mathcal{N}^*, \quad \text{Supp}(\varphi_{n,j}) = [nh, (n+1)h], \forall n \in \mathcal{N},$$

with $\mathcal{N}^* \coloneqq \mathcal{N} \setminus \{0\}$. In order to take into account periodicity, we also have

$$\text{Supp}(\varphi_{0,0}) = [0, h] \cup [L-h, L].$$

Moreover, we assume that the shape functions are obtained by translation, namely

(3.1)

$$\forall x \in [0,h],\, \forall n \in \mathcal{N}^*,\, \forall j \in \mathcal{R}^*, \quad \begin{cases} \varphi_{n,0}(x + n\,h) = \varphi_{0,0}(x) & \in \mathcal{P}^R([0,h]), \\ \varphi_{n,0}(x + (n-1)\,h) = \varphi_{1,0}(x) & \in \mathcal{P}^R([0,h]), \\ \varphi_{n,j}(x + n\,h) = \varphi_{0,j}(x) & \in \mathcal{P}^R([0,h]), \end{cases}$$

where $\mathcal{P}^R([0,h])$ denotes the set of polynomials of degree R on $[0,h]$ and with $\mathcal{R}^* \coloneqq \mathcal{R} \setminus \{0\}$, and where, by periodicity again, $\varphi_{0,0}(x + L - h) = \varphi_{1,0}(x)$, for $x \in [0,h]$. We introduce the set of Gauss-Lobatto points $\left\{\xi_j\right\}_{j=0}^{R}$, s.t. $\xi_j \in [0,1]$ for all $j \in \mathcal{R}$ and, by definition of shape functions, we have

$$\varphi_{m,i}((\xi_j + n)h) = \delta_{m\,n}\,\delta_{i\,j}, \ \forall i, j \in \mathcal{R}, \forall m, n \in \mathcal{N}.$$

By way of illustration, Lagrange basis functions for $R = 2$ are depicted in Figure 1. Then, $f_h, u_h \in \mathcal{V}_{h,R}$ can be rewritten as

$$f_h(x) = \sum_{n\in\mathcal{N}} \sum_{j\in\mathcal{R}} f_{n,j}\,\varphi_{n,j}(x), \quad u_h(x) = \sum_{n\in\mathcal{N}} \sum_{j\in\mathcal{R}} u_{n,j}\,\varphi_{n,j}(x),$$

Figure 1 Shape functions for quadratic Lagrange polynomial interpolation on Gauss-Lobatto points in $[0, L]$.

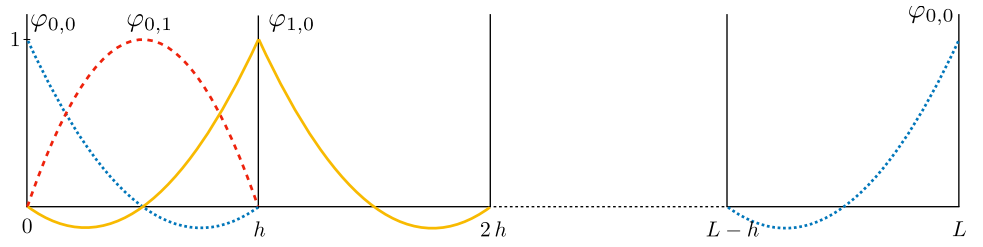

with coefficients

$$f_{n,j} \coloneqq f_h((\xi_j + n)h), \quad u_{n,j} \coloneqq u_h((\xi_j + n)h) \quad \forall j \in \mathcal{R}, \forall n \in \mathcal{N},$$

and an analogous decomposition holds for $v_h \in \mathcal{V}_{h,R}$. We can introduce an interpolation function of f_h defined as

$$\tilde{f}_h(x) = \frac{1}{N} \sum_{k \in \mathcal{N}} \Big(\sum_{j \in \mathcal{R}} \hat{f}_{k,j}\, e^{\frac{i2\pi(x - h\xi_j)k}{L}} \sum_{n \in \mathcal{N}} \varphi_{n,j}(x) \Big). \tag{3.2}$$

As a consequence of our definition, we obtain

$$\tilde{f}_h((\xi_j + n)h) = \frac{1}{N} \sum_{k \in \mathcal{N}} \hat{f}_{k,j}\, e^{\frac{i2\pi nk}{N}}, \ \forall j \in \mathcal{R}, \tag{3.3}$$

since $h\,N = L$. Eq. (3.3) represents a generalisation of Eq. (2.5) for higher-order spatial approximation. Therefore, the coefficients $\hat{f}_{k,j}$, for all $j \in \mathcal{R}$, can be computed by means of classical DFT. In particular, the following Proposition holds.

PROPOSITION 3.1. *Let f_h and $\tilde{f}_h$ belongs to $C^0_\sharp([0, L])$ be defined by Eq. (3.2). Let*

$$\tilde{f}_{n,j} \coloneqq \tilde{f}_h((\xi_j + n)h) \quad \forall j \in \mathcal{R}, \forall n \in \mathcal{N}.$$

Then, we have, for all j fixed in $\mathcal{R}$,

$$\begin{aligned} f_{n,j} = \tilde{f}_{n,j} &\iff \hat{f}_{k,j} = \sum_{n \in \mathcal{N}} f_{n,j}\, e^{-\frac{i2\pi nk}{N}}, \ \forall k \in \mathcal{N}, \\ &\iff f_{n,j} = \frac{1}{N} \sum_{k \in \mathcal{N}} \hat{f}_{k,j}\, e^{\frac{i2\pi nk}{N}}, \ \forall n \in \mathcal{N}. \end{aligned} \tag{3.4}$$

Proposition 3.1 is a straightforward consequence of Proposition 2.1 and Eq. (3.3). Following the approach in Section 2.2, we introduce the interpolation function of u_h,

$$\tilde{u}_{n,j} \coloneqq \tilde{u}_h((\xi_j + n)h) = \frac{1}{N} \sum_{k \in \mathcal{N}} \hat{u}_{k,j}\, e^{\frac{i2\pi nk}{N}}, \ \forall j \in \mathcal{R}, \tag{3.5}$$

where the coefficients $\hat{u}_{k,j}$ are given by

$$\hat{u}_{k,j} = \sum_{n \in \mathcal{N}} u_{n,j}\, e^{-\frac{i2\pi nk}{N}}, \ \forall k \in \mathcal{N}, \ \forall j \in \mathcal{R}. \tag{3.6}$$

As a consequence of Eqs. (3.5) and (3.6) and Proposition 3.1, we derive

$$u_{n,j} = \tilde{u}_{n,j}, \quad \forall n \in \mathcal{N},\ \forall j \in \mathcal{R}. \tag{3.7}$$

We now manipulate the bilinear forms in Eq. (2.2). If the same quadrature formula is used for each segment of size h, the bilinear form m_h in Eq. (2.2) can be rewrite

$$m_h(u_h, v_h) = \sum_{n\in\mathcal{N}} \int_{[nh,(n+1)h]}^{Q} u_h(x)\,\overline{v_h(x)}\,\mathrm{d}x = \sum_{n\in\mathcal{N}} \int_{[0,h]}^{Q} u_h(x+nh)\,\overline{v_h(x+nh)}\,\mathrm{d}x.$$

Consequently, by quadrature rule (Eq. (2.3)) and the definition of shape functions, we obtain

$$\int_{[0,h]}^{Q} u_h(x+nh)\,\overline{v_h(x+nh)}\,\mathrm{d}x = h\sum_{k=0}^{R_Q}\sum_{i,j=0}^{R} \omega_k \varphi_{0,i}(\eta_k\, h)\varphi_{0,j}(\eta_k\, h) u_{n,j}\,\overline{v_{n,i}},$$

where, for the sake of conciseness, we use the notations $\varphi_{0,R}(x) = \varphi_{1,0}(x)$, and also $u_{n,R} = u_{n+1,0}$, and by periodicity, $u_{N-1,R} = u_{N,0} = u_{0,0}$ (a same notation is used for $v_{n,i}$). Finally, one can show that

$$m_h(u_h, v_h) = \sum_{n\in\mathcal{N}}\sum_{i,j=0}^{R} \hat{m}_{i,j} u_{n,j}\,\overline{v_{n,i}},$$

where $\hat{m}_{i,i}$ denote the coefficients of the mass matrix in the reference element $[0, h]$. Similar treatment of the bilinear form a_h gives

$$a_h(u_h, v_h) = \sum_{n\in\mathcal{N}}\sum_{i,j=0}^{R} \hat{a}_{i,j} u_{n,j}\,\overline{v_{n,i}}.$$

Note that the coefficients $\hat{a}_{i,j}$ and $\hat{m}_{i,i}$ do not depend on the index n, as a consequence of the invariance of the discrete bilinear forms with respect to translations. This property is fundamental for the derivation of the symbol of the operator. Furthermore, due to the use of Gauss-Lobatto nodes both for the interpolation and the quadrature rule (i.e. $\{\eta_k\} = \{\xi_k\}$), the mass matrix is diagonal. This property, named mass lumping, is a fundamental feature of Spectral Element Methods (SEM), first proposed by [15]. We make this choice for the rest of the article. Consequently, we obtain

$$m_h(u_h, v_h) = \sum_{n\in\mathcal{N}}\sum_{i=0}^{R} \hat{m}_{i,i} u_{n,i}\,\overline{v_{n,i}},$$

and the algebraic system to solve is

$$\sum_{n\in\mathcal{N}}\sum_{i=0}^{R} \hat{m}_{i,i} u_{n,i}\,\overline{v_{n,i}} + \sum_{n\in\mathcal{N}}\sum_{i,j=0}^{R} \hat{a}_{i,j} u_{n,j}\,\overline{v_{n,i}} = \sum_{n\in\mathcal{N}}\sum_{i=0}^{R} \hat{m}_{i,i} f_{n,i}\,\overline{v_{n,i}}. \tag{3.8}$$

Since Eq. (2.2) must be true for any $v_h \in \mathcal{V}_h$, it must hold true for any choice of $v_{n,i}$, $v \in \mathcal{N},\ i \in \{0, 1, .., R\}$. In particular, for $v_{n,i} = \delta_{i\,q}\,\delta_{n\,\ell}$, with $q \in \mathcal{R}$ and $\ell \in \mathcal{N}$,

$$\hat{m}_{q,q}\, u_{l,q} + \sum_{j\in\mathcal{R}^*} \hat{a}_{q,j}\, u_{l,j} + \hat{a}_{q,0}\, u_{l,0} + \hat{a}_{q,R}\, u_{l+1,0} = \hat{m}_{q,q}\, f_{l,q}. \tag{3.9}$$

Note that Eq. (3.9) is still true when we replace $u_{l,j}$ by $\tilde{u}_{l,j}$ and $f_{l,j}$ by $\tilde{f}_{l,j}$, due to Eq. (3.7). Following the strategy of Section 2.2, we further replace $\tilde{u}_{l,j}$ by their expression in terms of $\hat{u}_{k,j}$ (Eq. (3.5)) and $\tilde{f}_{l,j}$ by their expression in terms of $\hat{f}_{k,j}$ (Eq. (3.3)), for all $j \in \mathcal{R}$ and observing that $\tilde{u}_{l,R} = \tilde{u}_{l+1,0}$ and $\tilde{f}_{l,R} = \tilde{f}_{l+1,0}$ by definition. Therefore, Eq. (3.9) becomes, $\forall q \in \mathcal{R}$,

$$\sum_{k\in\mathcal{N}} \left(\hat{m}_{q,q}\, \hat{u}_{k,q}\, e^{\frac{i2\pi k\ell}{N}} + \sum_{j\in\mathcal{R}^*} \hat{a}_{q,j}\, \hat{u}_{k,j}\, e^{\frac{i2\pi k\ell}{N}} + \big(\hat{a}_{q,0} + \hat{a}_{q,R}\, e^{\frac{i2\pi k}{N}}\big)\hat{u}_{k,0}\, e^{\frac{i2\pi k\ell}{N}} \right) = \sum_{k\in\mathcal{N}} \hat{m}_{q,q}\, \hat{f}_{k,q}\, e^{\frac{i2\pi k\ell}{N}}. \tag{3.10}$$

In particular, if $q = 0$, we obtain

$$\sum_{k\in\mathcal{N}} \left(\hat{m}_{0,0}\, \hat{u}_{k,0}\, e^{\frac{i2\pi k\ell}{N}} + \sum_{j\in\mathcal{R}^*} \hat{a}_{0,j}\, \hat{u}_{k,j}\, e^{\frac{i2\pi k\ell}{N}} + \big(\hat{a}_{0,0} + \hat{a}_{0,R}\, e^{\frac{i2\pi k}{N}}\big)\hat{u}_{k,0}\, e^{\frac{i2\pi k\ell}{N}} \right) = \sum_{k\in\mathcal{N}} \hat{m}_{0,0}\, \hat{f}_{k,0}\, e^{\frac{i2\pi k\ell}{N}}. \tag{3.11}$$

Furthermore, if $q = R$, Eq. (3.10) can be rewritten as

$$\sum_{k\in\mathcal{N}} \left(\hat{m}_{R,R}\, \hat{u}_{k,0}\, e^{\frac{i2\pi k\ell}{N}} + \sum_{j\in\mathcal{R}^*} \hat{a}_{R,j}\, \hat{u}_{k,j}\, e^{\frac{i2\pi (k-1)\ell}{N}} + \big(\hat{a}_{R,0}\, e^{\frac{-i2\pi k}{N}} + \hat{a}_{R,R}\big)\hat{u}_{k,0}\, e^{\frac{i2\pi k\ell}{N}} \right) = \sum_{k\in\mathcal{N}} \hat{m}_{R,R}\, \hat{f}_{k,0}\, e^{\frac{i2\pi k\ell}{N}}, \tag{3.12}$$

since Eq (3.6) and $u_{n,R} = u_{n+1,0}$ implies that $\hat{u}_{k,R} = \hat{u}_{k+1,0}$ and $\hat{f}_{k,R} = \hat{f}_{k+1,0}$. Let us now define the vectors $\underline{\hat{U}}_k, \underline{\hat{F}}_k \in \mathbb{C}^R$, such that

$$\underline{\hat{U}}_k = (\hat{u}_{k,0}\,, \hat{u}_{k,1}, .., \hat{u}_{k,R-1})^T, \quad \underline{\hat{F}}_k = (\hat{f}_{k,0}\,, \hat{f}_{k,1}, .., \hat{f}_{k,R-1})^T,$$

and the matrices $\boldsymbol{\mathcal{A}}_k, \boldsymbol{\mathcal{M}} \in \mathbb{C}^{R\times R}$ such that

$$\boldsymbol{\mathcal{A}}_k = \begin{bmatrix} \mathrm{a}_k & \underline{\mathcal{B}}_k \\ \underline{\mathcal{B}}_k^* & \mathring{\boldsymbol{\mathcal{A}}} \end{bmatrix}, \quad \boldsymbol{\mathcal{M}} = \begin{bmatrix} \mathcal{M} & 0 \\ 0 & \mathring{\boldsymbol{\mathcal{M}}} \end{bmatrix}, \tag{3.13}$$

where $\mathrm{a}_k,\ \mathcal{M} \in \mathbb{C}$, the vector $\underline{\mathcal{B}}_k$ belongs to $\mathbb{C}^{R-1}$ and the matrices $\mathring{\boldsymbol{\mathcal{A}}}$, $\mathring{\boldsymbol{\mathcal{M}}}$ belong to $\mathbb{C}^{(R-1)\times(R-1)}$. They are given by

$$\mathrm{a}_k = \hat{a}_{0,0} + \hat{a}_{R,R} + 2\,\hat{a}_{0,R}\,\cos(2\pi k/N), \quad \mathcal{M} = \hat{m}_{0,0} + \hat{m}_{R,R},$$

and

$$\mathcal{B}_{k,q} = \hat{a}_{0,q} + \hat{a}_{R,q}\, e^{i2\pi k/N}, \quad \mathring{\boldsymbol{\mathcal{M}}}_{q\,q^*} = \hat{m}_{q,q^*}\,\delta_{q\,q^*}, \quad \mathring{\boldsymbol{\mathcal{A}}}_{q\,q^*} = \hat{a}_{q,q^*},\ q, q^* \in \mathcal{R}^*.$$

Thereupon, Eqs. (3.10), (3.11) and (3.12) can be rewritten in compact form as

$$\sum_{k\in\mathcal{N}} e^{\frac{i2\pi k\ell}{N}} (\rho\,\boldsymbol{\mathcal{M}} + \boldsymbol{\mathcal{A}}_k)\,\underline{\hat{U}}_k = \sum_{k\in\mathcal{N}} e^{\frac{i2\pi k\ell}{N}} \boldsymbol{\mathcal{M}}\,\underline{\hat{F}}_k,\ \forall l \in \mathcal{N}. \tag{3.14}$$

Figure 2 Redistribution of the source term in matrix form. Row index corresponds to the element, column index refers to the Gauss-Lobatto node in the reference element.

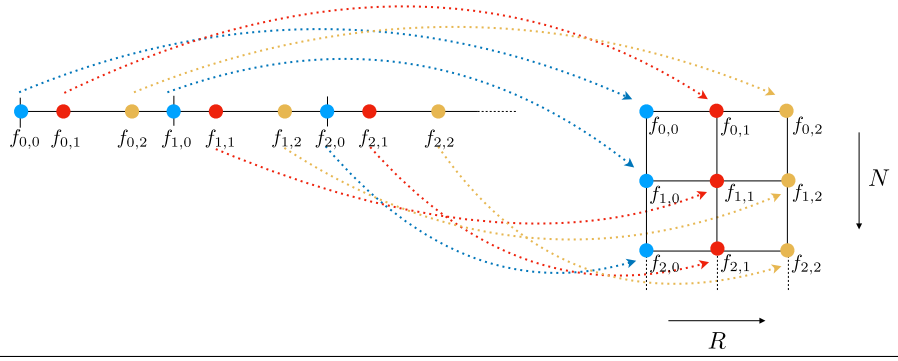

By orthogonality of the factors $e^{\frac{i2\pi kl}{N}}$ (Eq. (2.6)), we can further simplify Eq. (3.14),

$$(\rho\,\boldsymbol{\mathcal{M}} + \boldsymbol{\mathcal{A}}_k)\,\underline{\hat{U}}_k = \boldsymbol{\mathcal{M}}\,\underline{\hat{F}}_k,\ \forall k \in \mathcal{N}.$$

Ultimately, the solution $\hat{U}_k$, for every frequency $k \in \mathcal{N}$, is computed as

$$\underline{\hat{U}}_k = \boldsymbol{\mathcal{S}}_k^{-1}\,\underline{\hat{F}}_k\ \forall k \in \mathcal{N}, \tag{3.15}$$

where the symbol of the operator $\boldsymbol{\mathcal{S}}_k$ reads

$$\boldsymbol{\mathcal{S}}_k = (\rho\,\mathbf{I} + \boldsymbol{\mathcal{M}}^{-1}\,\boldsymbol{\mathcal{A}}_k).$$

The algorithm. In order to solve (3.8), we can derive an algorithm based on Eqs. (3.4), (3.15) and (3.6). The main steps of this algorithm read:

1. Perform a DFT of the discrete source term for each order j fixed in $\mathcal{R}$

$$\hat{f}_{k,j} = \sum_{n\in\mathcal{N}} f_{n,j}\,e^{-\frac{i2\pi nk}{N}},\ \forall k \in \mathcal{N};$$

2. Apply the inverse symbol of the operator

$$\underline{\hat{U}}_k = \boldsymbol{\mathcal{S}}_k^{-1}\,\underline{\hat{F}}_k,\ \forall k \in \mathcal{N}; \tag{3.16}$$

3. Perform an inverse DFT for each order j fixed in $\mathcal{R}$

$$u_{n,j} = \frac{1}{N}\sum_{k\in\mathcal{N}} \hat{u}_{k,j}\,e^{\frac{i2\pi nk}{N}},\ \forall n \in \mathcal{N}.$$

A crucial aspect of this method concerns the definition of an efficient algorithm to compute the coefficients $f_{n,j}$ and $\hat{f}_{k,j}$. To this end, we re-organise the source term vector in matrix form, in which the row index corresponds to the element, whereas the column index refers to the Gauss-Lobatto point in the reference element of size h. Then, the terms $\hat{f}_{k,j}$ are obtained by DFT column by column (using the FFT algorithm). See Figure 2 for a schematic illustration of the procedure.

Inversion of the symbol by SVD. In this section we anticipate the difficulties that will be encountered in multiple dimensions, namely the inversion of the symbol of the operator $\boldsymbol{\mathcal{S}}_k$ in Eq. (3.16). We now derive a pseudo-explicit inversion of this matrix by means of Singular Value Decomposition (SVD). For this purpose, let us denote by $\left\{\underline{V}_{k,i}, \lambda_{k,i}\right\}_{i\in\mathcal{R}}$ the set of eigenvectors and eigenvalues of $\boldsymbol{\mathcal{S}}_k$. They satisfy the generalised eigenvalue problem $\boldsymbol{\mathcal{S}}_k \underline{V}_{k,i} = \lambda_{k,i} \boldsymbol{\mathcal{M}} \underline{V}_{k,i}$ for all $i \in \mathcal{R}$. Since $\boldsymbol{\mathcal{S}}_k$ is hermitian and positive-definite, all eigenvalues $\lambda_{k,i}$ are positive and real for all $k > 0$, and all eigenvectors $\underline{V}_{k,i}$ are orthonormal with respect to the scalar product by $\boldsymbol{\mathcal{M}}$, i.e.

$$\underline{V}^*_{k,j} \boldsymbol{\mathcal{M}} \underline{V}_{k,i} = \delta_{ij}, \ \forall i, j \in \mathcal{R}.$$

After some standard algebra, we obtain

$$\boldsymbol{\mathcal{S}}_k = \sum_{i\in\mathcal{R}} \lambda_{k,i} \underline{V}_{k,i} \underline{V}^*_{k,i} \boldsymbol{\mathcal{M}} \implies \boldsymbol{\mathcal{S}}_k^{-1} = \sum_{i\in\mathcal{R}} \lambda_{k,i}^{-1} \underline{V}_{k,i} \underline{V}^*_{k,i} \boldsymbol{\mathcal{M}}.$$

Therefore, Eq. (3.16) can be rewritten as

$$\underline{\hat{U}}_k = \sum_{i\in\mathcal{R}} \lambda_{k,i}^{-1} \underline{V}_{k,i} \underline{V}^*_{k,i} \boldsymbol{\mathcal{M}} \underline{\hat{F}}_k. \tag{3.17}$$

At this stage, Eq. (3.17) requires the same computational cost as Eq. (3.16), since the computation of the eigenvalues and eigenvectors of a matrix implies the same number of operations as the multiplication by an inverse matrix. Nevertheless, we will show in Section 4 that the generalisation to higher dimensions becomes very efficient, due to tensorisation.

3.2. Neumann and Dirichlet Boundary conditions. When linear interpolation is used, it is standard to use, in the definition of the interpolation function (2.5), the Discrete Sine Transform (DST) for Dirichlet BCs, or Discrete Cosine Transform (DCT) for Neumann BCs. If a high-order approximation is used, It is not possible to use DCT or DST and we explicitly "double" the computational domain and the discrete source term f_h in order to extend it into a periodic one and perform DFT. According to the BC imposed, we perform an even (for Neumann BCs) or odd (for Dirichlet BCs) extension of our source term (that is set to 0 at the end-points of the interval for antisymmetric extensions). See Figure 3 for a graphical illustration of this procedure in one-dimension. Therefore, we need to take into account $2N$ frequencies for each direction, instead of N frequencies for the periodic case. However, thanks to symmetry properties of the DFT, we are able to restrict most operations to $N + 1$ frequencies, as shown in what follows.
Henceforth, we extend the analysis for a one-dimensional, complex-valued discrete source term f_h. Note that, after doubling the computational domain and performing an even (or odd) extension of the source term, depending on the BCs considered, the sequence $\left\{f_{n,R-j}\right\}_{n\in\mathcal{N},j\in\mathcal{R}}$ satisfies, for any given $n \in \mathcal{N}$,

$$\begin{cases} f_{n,R-j} = f_{2N-n-1,j}, & \text{if } j \in \mathcal{R}^*, \\ f_{n,0} = f_{2N-n,0}, \end{cases} \tag{3.18}$$

for an even extension, and

$$\begin{cases} f_{n,R-j} = -f_{2N-n-1,j}, & \text{if } j \in \mathcal{R}^*, \\ f_{n,0} = -f_{2N-n,0}, \end{cases} \tag{3.19}$$

Figure 3 Illustration of a periodic extension of a discrete, one-dimensional function at Gauss-Lobatto nodes. Left: comparison between original function and its even expansion (for Neumann BCs); right: comparison between original function and its odd expansion (for Dirichlet BCs). Gauss-Lobatto nodes for N=2 elements, 5^{th}-Order Lagrange polynomials.

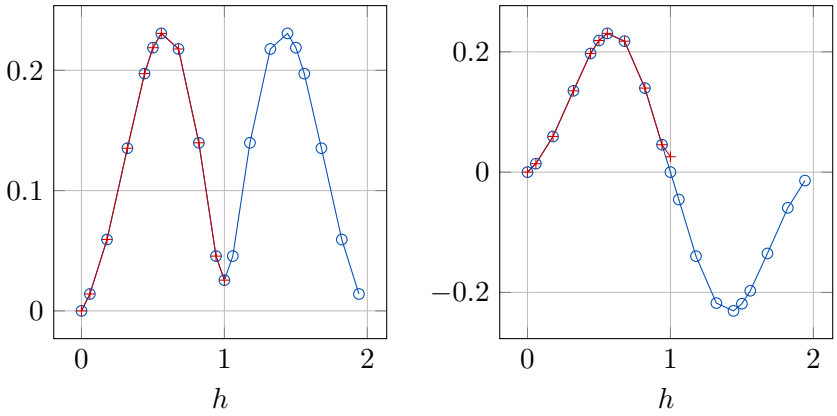

for an odd extension. Henceforth, we use the symbol $\pm$ for the sake of conciseness, where $+$ is associated with Neumann conditions, whereas $-$ corresponds to Dirichlet conditions. We define the coefficients $\hat{f}_{k,j}$ following Eq. (3.4). Given $j \in \mathcal{R}$, they read

$$\hat{f}_{k,j} = \sum_{n=0}^{2N-1} f_{n,j}\, e^{-\frac{i\pi nk}{N}}, \quad \forall k \in \{0, 1, .., 2N-1\}.$$

From the properties of the sequence $\{f_{n,j}\}_{n\in\mathcal{N},j\in\mathcal{R}}$ we can deduce some symmetry properties of the coefficients $\hat{f}_{k,j}$, as stated in the following lemma. These properties allow to reduce the number of frequencies considered for the construction of the symbol of the operator. Due to the use of high-order polynomial interpolation, this symmetry is not trivial.

LEMMA 3.2. *Let $\{f_{n,j}\}_{n\in\mathcal{N},j\in\mathcal{R}}$ be a complex-valued sequence. If the sequence satisfies Eq. (3.18) or Eq. (3.19), the coefficients $\hat{f}_{k,j}$ read, $\forall k \in \mathcal{N}^*$*

$$\begin{cases} \hat{f}_{2N-k,j} = \pm e^{\frac{-i\pi k}{N}} \hat{f}_{k,R-j}, & \text{if } \ j \in \mathcal{R}^*, \\ \hat{f}_{2N-k,0} = \pm \hat{f}_{k,0}, \end{cases} \tag{3.20}$$

with the established convention for the plus and minus signs.

Proof. Let us consider an even extension of the discrete source term, and fix $j \in \mathcal{R}^*$. On the one hand, due to Eq. (3.18), Eq. (3.19) and Lemma 3.2, we are able to retrieve that, for $k \in \mathcal{N} \cup \{N\}$,

$$\begin{aligned} \hat{f}_{k,R-j} &= \sum_{n=0}^{2N-1} f_{n,R-j}\, e^{-\frac{i\pi nk}{N}} = \sum_{n=0}^{2N-1} f_{2N-n-1,j}\, e^{-\frac{i\pi nk}{N}} \\ &= \sum_{m=0}^{2N-1} f_{m,j}\, e^{\frac{-i2N\pi k}{N}} e^{\frac{i\pi mk}{N}} e^{\frac{i\pi k}{N}} = e^{\frac{i\pi k}{N}} \sum_{m=0}^{2N-1} f_{m,j}\, e^{\frac{i\pi mk}{N}}. \end{aligned}$$

On the other hand, due to a standard property of DFT, we have that

$$\hat{f}_{2N-k,j} = \sum_{m=0}^{2N-1} f_{m,j}\, e^{\frac{-i\pi m(2N-k)}{N}} = \sum_{m=0}^{2N-1} f_{m,j}\, e^{\frac{i\pi mk}{N}},\ \forall j \in \mathcal{R}.$$

Hence, we deduce that

$$\hat{f}_{k,R-j} = e^{\frac{i\pi k}{N}} \hat{f}_{2N-k,j}. \tag{3.21}$$

In addition, for $j = 0$ and $k \in \mathcal{N} \cup \{N\}$, we obtain

$$\begin{aligned} \hat{f}_{k,0} &= \sum_{n=0}^{2N-1} f_{n,0}\, e^{-\frac{i\pi nk}{N}} = \sum_{n=0}^{2N-1} f_{2N-n,0}\, e^{-\frac{i\pi nk}{N}} \\ &= \sum_{m=1}^{2N} f_{m,0}\, e^{\frac{-i2N\pi k}{N}} e^{\frac{i\pi mk}{N}} = \sum_{m=0}^{2N-1} f_{m,0}\, e^{\frac{i\pi mk}{N}} \\ &= \hat{f}_{2N-k,0}, \end{aligned} \tag{3.22}$$

since, by periodicity, $f_{2N,0} = f_{0,0}$. The proof for odd extension of the discrete source term is analogous. ∎

Furthermore, we state the following proposition:

PROPOSITION 3.3. *Let us consider Problem (2.1), with $\Omega = [0, 2L]$. Then, if the source term f is periodic of period L and even (odd), the solution u is endowed with the same properties, i.e. it is periodic of period L and even (odd).*

Note that Proposition 3.3 also holds true for the discrete problem (3.8), and f_h, u_h. From Lemma 3.2 and Proposition 3.3, we deduce that the discrete solution u_h satisfies Eq.(3.20). For this reason, we can construct an efficient algorithm for the solution of a Poisson problem by HO-DFT that consists in three steps:

1. Perform a DFT of the discrete source term for each order j fixed in $\mathcal{R}^*$

$$\hat{f}_{k,j} = \sum_{n=0}^{2N-1} f_{n,j}\, e^{-\frac{i\pi nk}{N}},\ \forall k \in \mathcal{N} \cup \{N\};$$

   with $f_{n,j}$ given by (3.19) for $n \geqslant N$.
2. Apply the inverse symbol of the operator for each frequency

$$\hat{\underline{U}}_k = \boldsymbol{\mathcal{S}}_k^{-1}\, \hat{\underline{F}}_k,\ \forall k \in \mathcal{N} \cup \{N\};$$

3. Perform an inverse DFT for each order j fixed in $\mathcal{R}^*$

$$u_{n,j} = \frac{1}{2N} \sum_{k=0}^{2N-1} \hat{u}_{k,j}\, e^{\frac{i\pi nk}{N}},\ \forall n \in \mathcal{N} \cup \{N\}.$$

   with $\hat{u}_{k,j}$ given by (3.20) for $k \geqslant N+1$.

This algorithm relies on the evaluation of the symbol of the operator of the first $N+1$ frequencies only. Note, however, that the standard implementation of DFT (or its inverse) by FFT algorithm implies the evaluation of all 2N frequencies. However, in Step 2, only $N+1$ inversions of the symbol are required. We will show in what follows that in multi-dimensions it is possible to optimise Steps 1 and 3, by considering an *ad hoc* extension of the sequence "dimension by dimension" when the FFT (or its inverse) is performed.

Remark Note that the $\boldsymbol{\mathcal{A}}_k$ are all invertible, except for the case $k = 0$. Indeed, if $k = 0$, the constant vector is an eigenvector of $\boldsymbol{\mathcal{A}}_0$ associated with the eigenvalue 0. Therefore, if $\rho = 0$, then $\boldsymbol{\mathcal{S}}_k = \boldsymbol{\mathcal{A}}_k$ and $\underline{\hat{U}}_k$ is computed using a pseudoinverse of $\boldsymbol{\mathcal{A}}_k$, i.e.

$$\underline{\hat{U}}_k = \sum_{\substack{i\in\mathcal{R}\\ \lambda_{k,i}\neq 0}} \lambda_{k,i}^{-1}\, \underline{V}_{k,i}\, \underline{V}_{k,i}^{*}\, \boldsymbol{\mathcal{M}}\, \underline{\hat{F}}_k. \tag{3.23}$$

Eq. (3.23) corresponds to setting the mean value of the solution equal to zero.

4. Extension to higher dimensions. The generalisation to two (or higher) dimensions is performed by tensorisation from the one-dimensional case. Therefore, most of the properties are directly inherited from the one-dimensional case, and we do not provide the proofs, for the sake of conciseness. Henceforth, we denote by $d > 1$ the dimension of the computational domain.

4.1. Periodic boundary conditions. First, let us define $\mathcal{N}^d = \{0, 1, .., N-1\}^d$ and $\mathcal{R}^d = \{0, 1, .., R-1\}^d$. We introduce the set of points in the reference element $[0, 1]^d$ as

$$\underline{\xi}_{\mathbf{j}} = [\xi_{j_1}, \xi_{j_2}, .., \xi_{j_r}],$$

where ξ_i corresponds to a 1-D Gauss-Lobatto point for all $i \in \mathcal{R}$, and $\mathbf{j}$ is a multi-index in $\mathcal{R}^d$. Let us introduce the multi-index $\mathbf{n} = [n_1, n_2, .., n_d] \in \mathcal{N}^d$. Then, the d-dimensional shape functions defined on $\underline{x} = [x_1, x_2, .., x_d] \in [0, L]^d$ read

$$\Phi_{\mathbf{n},\mathbf{j}}(\underline{x}) = \prod_{r=1}^{d} \varphi_{n_r,j_r}(x_r), \tag{4.1}$$

where $\varphi_{n_r,j_r}(x_r)$ are shape functions defined as in Section (3.1). Therefore, the shape functions $\Phi_{\mathbf{n},\mathbf{j}}$ satisfy, for all $\mathbf{p} \in \mathcal{R}^d$, and all $\mathbf{m} \in \mathcal{N}^d$,

$$\begin{aligned}\Phi_{\mathbf{m},\mathbf{p}}((\underline{\xi}_{\mathbf{j}} + \mathbf{n})h) &= \Phi_{\mathbf{m},\mathbf{p}}((\xi_{j_1} + n_1)h, (\xi_{j_2} + n_2)h, .., (\xi_{j_d} + n_d)h)\\ &= \prod_{r=1}^{d} \delta_{m_r\, n_r}\, \varphi_{n_r,p_r}(\xi_{j_r}) = \prod_{r=1}^{d} \delta_{m_r\, n_r}\, \delta_{p_r\, j_r}.\end{aligned}$$

For simplicity of notation, we denote

$$\sum_{\mathbf{n}} \coloneqq \sum_{n_1=0}^{N-1}\sum_{n_2=0}^{N-1}\cdots\sum_{n_d=0}^{N-1}, \quad \sum_{\mathbf{j}} \coloneqq \sum_{j_1=0}^{R-1}\sum_{j_2=0}^{R-1}\cdots\sum_{j_d=0}^{R-1}, \quad \sum_{\mathbf{n},\mathbf{j}} \coloneqq \sum_{\mathbf{n}}\sum_{\mathbf{j}},$$

moreover for any vector $V \in \mathbb{C}^{R^d}$ $V(\mathbf{i})$ its $\mathbf{i}$th element without assuming a specific one-dimensional re-ordering of the degree of freedoms with respect to the multi-indices. A similar strategy is used for matrices $\boldsymbol{V} \in \mathbb{C}^{R^d \times R^d}$, its element on the $\mathbf{i}$th line and $\mathbf{j}$th column is denoted $\boldsymbol{V}(\mathbf{i}, \mathbf{j})$. From Eq. (4.1) we derive the following decomposition for the discrete source term f_h and the discrete solution u_h:

$$f_h(\underline{x}) = \sum_{\mathbf{n},\mathbf{j}} f_{\mathbf{n},\mathbf{j}}\, \Phi_{\mathbf{n},\mathbf{j}}(\underline{x}), \quad u_h(\underline{x}) = \sum_{\mathbf{n},\mathbf{j}} u_{\mathbf{n},\mathbf{j}}\, \Phi_{\mathbf{n},\mathbf{j}}(\underline{x}),$$

with

$$f_{\mathbf{n},\mathbf{j}} \coloneqq f_h\big((\underline{\xi}_{\mathbf{j}} + \mathbf{n})h\big) \quad u_{\mathbf{n},\mathbf{j}} \coloneqq u_h\big((\underline{\xi}_{\mathbf{j}} + \mathbf{n})h\big), \quad \forall \mathbf{n} \in \mathcal{N}^d,\, \forall \mathbf{j} \in \mathcal{R}^d.$$

With these notations the algebraic problem that must be solved reads: find $\{u_{\mathbf{n},\mathbf{i}}\}$ such that

$$\sum_{\mathbf{n}} \sum_{\mathbf{j}} \hat{m}_{\mathbf{j},\mathbf{j}} u_{\mathbf{n},\mathbf{i}}\, \overline{v_{\mathbf{n},\mathbf{i}}} + \sum_{\mathbf{n}} \sum_{\mathbf{i}} \sum_{\mathbf{j}} \hat{a}_{\mathbf{i},\mathbf{j}} u_{\mathbf{n},\mathbf{j}}\, \overline{v_{\mathbf{n},\mathbf{i}}} = \sum_{\mathbf{n}} \sum_{\mathbf{i}} \hat{m}_{\mathbf{i},\mathbf{i}} f_{\mathbf{n},\mathbf{i}}\, \overline{v_{\mathbf{n},\mathbf{i}}}, \tag{4.2}$$

for all $\{v_{\mathbf{n},\mathbf{i}}\}$, where $\{\hat{m}_{\mathbf{j},\mathbf{j}}\}$ and $\{\hat{a}_{\mathbf{i},\mathbf{j}}\}$ correspond to the elements of the mass and stiffness matrices, respectively, computed on the multidimensional reference element $[0,h]^d$. Now let $\mathbf{k} \in \mathcal{N}^d$. Since the source term is periodic in $[0,L]^d$, we can generalise the definition of an interpolation function (3.2) for higher dimensions as

$$\tilde{f}_h(\underline{x}) = \frac{1}{N^d} \sum_{\mathbf{k}} \left(\sum_{\mathbf{j}} \hat{f}_{\mathbf{k},\mathbf{j}}\, e^{\frac{i2\pi(\underline{x} - h\underline{\xi}_{\mathbf{j}})\cdot\mathbf{k}}{L}} \sum_{\mathbf{n}} \varphi_{\mathbf{n},\mathbf{j}}(\underline{x}) \right), \tag{4.3}$$

with $h\,N = L$ and

$$e^{\frac{i2\pi(\underline{x} - h\underline{\xi}_{\mathbf{j}})\cdot\mathbf{k}}{L}} = e^{\frac{i2\pi(x_1 - h\xi_{j_1})\,k_1}{L}}\, e^{\frac{i2\pi(x_2 - h\xi_{j_2})\,k_2}{L}} \cdots e^{\frac{i2\pi(x_d - h\xi_{j_d})\,k_d}{L}}.$$

Note that this formula can be easily extended to more general, regular meshes by considering a different length L depending on the direction. Eq. (4.3) is a generalisation of Eq. (3.2) to the multi-dimensional case. Therefore, the coefficients $\hat{f}_{k,j},\ \forall j \in \mathcal{R}$, can be computed by DFT, as stated in the following proposition.

PROPOSITION 4.1. *Let $f_h \in C^0_\sharp([0,L]^d)$ and $\tilde{f}_h \in C^0_\sharp([0,L]^d)$ defined by Eq. (4.3). Let us denote*

$$\tilde{f}_{\mathbf{n},\mathbf{j}} \coloneqq \tilde{f}_h\big((\underline{\xi}_{\mathbf{j}} + \mathbf{n})h\big) \quad \forall \mathbf{j} \in \mathcal{R}^d,\ \forall \mathbf{n} \in \mathcal{N}^d.$$

Then, for all $\mathbf{j}$ fixed in $\mathcal{R}^d$,

$$\begin{aligned} f_{\mathbf{n},\mathbf{j}} = \tilde{f}_{\mathbf{n},\mathbf{j}} \iff \hat{f}_{\mathbf{k},\mathbf{j}} &= \sum_{\mathbf{n}} f_{\mathbf{n},\mathbf{j}}\, e^{\frac{-i2\pi\mathbf{n}\cdot\mathbf{k}}{N}},\ \forall \mathbf{k} \in \mathcal{N}^d, \\ &\iff f_{\mathbf{n},\mathbf{j}} = \frac{1}{N^d} \sum_{\mathbf{k}} \hat{f}_{\mathbf{k},\mathbf{j}}\, e^{\frac{i2\pi\mathbf{n}\cdot\mathbf{k}}{N}},\ \forall \mathbf{n} \in \mathcal{N}^d. \end{aligned} \tag{4.4}$$

Similarly, we introduce the interpolation function of the discrete solution u_h such that, for all $\mathbf{j} \in \mathcal{R}^d$ fixed,

$$\tilde{u}_{\mathbf{n},\mathbf{j}} \coloneqq \tilde{u}_h\big((\xi_{\mathbf{j}} + \mathbf{n})h\big) = \frac{1}{N^d} \sum_{\mathbf{k}} \hat{u}_{\mathbf{k},\mathbf{j}}\, e^{\frac{i2\pi\mathbf{n}\cdot\mathbf{k}}{N}},\ ,\forall \mathbf{n} \in \mathcal{N}^d, \tag{4.5}$$

where

$$\hat{u}_{\mathbf{k},\mathbf{j}} = \sum_{\mathbf{n}} u_{\mathbf{n},\mathbf{j}}\, e^{-\frac{i2\pi\mathbf{n}\cdot\mathbf{k}}{N}},\ \forall \mathbf{k} \in \mathcal{N}^d. \tag{4.6}$$

Due to Eqs. (4.5) and (4.6) as well as Property 4.1, we retrieve

$$u_{\mathbf{n},\mathbf{j}} = \tilde{u}_{\mathbf{n},\mathbf{j}}, \quad \forall \mathbf{n} \in \mathcal{N}^d, \forall \mathbf{j} \in \mathcal{R}^d.$$

Then with by similar process as in the one-dimensional case, it is possible to show that, solving (4.2), is equivalent to solve

$$\underline{\hat{U}}_{\mathbf{k}} = \boldsymbol{\mathcal{S}}_{\mathbf{k}}^{-1}\, \underline{\hat{F}}_{\mathbf{k}}, \qquad \forall \mathbf{k} \in \mathcal{N}^d,$$

where $\underline{\hat{U}}_{\mathbf{k}}(\mathbf{j}) = \hat{u}_{\mathbf{k},\mathbf{j}}$ and $\underline{\hat{F}}_{\mathbf{k}}(\mathbf{j}) = \hat{f}_{\mathbf{k},\mathbf{j}}$ and where the matrix $\boldsymbol{\mathcal{S}}_{\mathbf{k}}$ will be given by Proposition 4.2 below. As a straightforward generalisation of the one-dimensional case, the main steps of the algorithm to solve (4.2) read:

1. Perform a DFT of the discrete source term for each order $\mathbf{j}$ fixed in $\mathcal{R}^d$

$$\hat{f}_{\mathbf{k},\mathbf{j}} = \sum_{\mathbf{n}} f_{\mathbf{n},\mathbf{j}}\, e^{\frac{-i2\pi \mathbf{n}\cdot\mathbf{k}}{N}}, \ \forall \mathbf{k} \in \mathcal{N}^d;$$

2. Solve for each frequency $\mathbf{k} \in \mathcal{N}^d$

$$\boldsymbol{\mathcal{S}}_{\mathbf{k}}\, \underline{\hat{U}}_{\mathbf{k}} = \underline{\hat{F}}_{\mathbf{k}}; \tag{4.7}$$

3. Perform an inverse DFT for each order $\mathbf{j}$ fixed in $\mathcal{R}^d$

$$u_{\mathbf{n},\mathbf{j}} = \frac{1}{N^d} \sum_{\mathbf{k}} \hat{u}_{\mathbf{k},\mathbf{j}}\, e^{\frac{i2\pi \mathbf{n}\cdot\mathbf{k}}{N}}, \ \forall \mathbf{n} \in \mathcal{N}^d.$$

We emphasise that the multi-dimensional DFT is implemented recursively from the one-dimensional DFT. Furthermore, Step 2 must be implemented with care. In fact, one possibility is to inverse the symbol $\boldsymbol{\mathcal{S}}_{\mathbf{k}}$ for each frequency, and then perform a matrix-vector multiplication to obtain $\underline{\hat{U}}_{\mathbf{k}}$. Note, however, that such an algorithm would imply a substantial computational cost. To give an idea, in 2-D the matrix inversion would require $O(R^6)$ operations ($O(R^{3d})$ in general), while matrix-vector multiplication requires $O(R^4)$ operations. In what follows, we propose a method that requires neither matrix inversion nor storage and drastically reduces the complexity of the algorithm, based on SVD and tensorisation.

For the sake of conciseness, we denote $\boldsymbol{\mathcal{N}}_k = \boldsymbol{\mathcal{M}}^{-1}\, \boldsymbol{\mathcal{A}}_k$, with $\boldsymbol{\mathcal{M}}$ and $\boldsymbol{\mathcal{A}}_k$ associated with the 1-D case, and defined in Eq. (3.13). We also can rewrite the one-dimensional symbol $\boldsymbol{\mathcal{S}}_k \coloneqq \rho\, \mathbf{I} + \boldsymbol{\mathcal{N}}_k$, with $\mathbf{I}$ the identity matrix of size $R \times R$. The result below is proven in [8].

Proposition 4.2.

$$\boldsymbol{\mathcal{S}}_{\mathbf{k}}(\boldsymbol{\ell}, \mathbf{m}) = \rho \prod_{r=1}^{d} \delta_{l_r\, m_r} + \sum_{r=1}^{d} \boldsymbol{\mathcal{N}}_{k_r}(\ell_r, m_r) \prod_{q \neq r} \delta_{\ell_q\, m_q}. \tag{4.8}$$

For example, when $d = 2$, the symbol reads

$$\boldsymbol{\mathcal{S}}_{\mathbf{k}}(\boldsymbol{\ell}, \mathbf{m}) = \rho\, \delta_{l_1\, m_1}\, \delta_{l_2\, m_2} + \boldsymbol{\mathcal{N}}_{k_1}(\ell_1, m_1)\, \delta_{\ell_2\, m_2} + \boldsymbol{\mathcal{N}}_{k_2}(\ell_2, m_2)\, \delta_{\ell_1\, m_1}.$$

This result is a direct consequence of the use of the Gauss-Lobatto nodes for quadrature formulae. Due to Proposition 4.2, it is possible to compute the eigenvalues and eigenvectors of the symbol $\boldsymbol{\mathcal{S}}_{\mathbf{k}}$ starting from eigenvalues and eigenvectors of the matrix $\boldsymbol{\mathcal{N}}_k$. Given $\mathbf{k} \in \mathcal{N}^d$, we denote $\left\{\lambda_{\mathbf{k},\mathbf{i}}, \underline{V}_{\mathbf{k},\mathbf{i}}\right\}_{\mathbf{i} \in \mathcal{R}^d}$ the set of eigenvalues and eigenvectors of $\boldsymbol{\mathcal{S}}_{\mathbf{k}}$ such that

$$\boldsymbol{\mathcal{S}}_{\mathbf{k}}\, \underline{V}_{\mathbf{k},\mathbf{i}} = \lambda_{\mathbf{k},\mathbf{i}}\, \underline{V}_{\mathbf{k},\mathbf{i}}, \quad \forall \mathbf{k} \in \mathcal{N}^d, \ \forall \mathbf{i} \in \mathcal{R}^d.$$

When $d = 2$ they are given in [8] and reads

$$\begin{cases} \lambda_{\mathbf{k},\mathbf{i}} = \rho + \nu_{k_1,i_1} + \nu_{k_2,i_2}, \\ \underline{V}_{\mathbf{k},\mathbf{i}} = \underline{W}_{k_1,i_1} \otimes \underline{W}_{k_2,i_2}, \end{cases}$$

where $\otimes$ denotes the tensor product and where $\{\nu_{k,i}, \underline{W}_{k,i}\}$ are the eigenvalues and corresponding eigenvectors of $\boldsymbol{\mathcal{N}}_{k_r}$. This tensorial structure is in fact general, as stated by the Corollary below (which proof is very algebraic but simple and is omitted).

COROLLARY 4.3. *Let* $\left\{\nu_{k_r,i_r}, \underline{W}_{k_r,i_r}\right\}_{i_r \in \mathcal{R}}$ *be the eigenvalues and eigenvectors of* $\boldsymbol{\mathcal{N}}_{k_r}$, $r \in \{1, 2, .., d\}$. *Then,*

$$\begin{cases} \lambda_{\mathbf{k},\mathbf{i}} = \rho + \displaystyle\sum_{r=1}^{d} \nu_{k_r,i_r}, \quad \forall \mathbf{i} \in \mathcal{R}^d, \\ V_{\mathbf{k},\mathbf{i}}(\mathbf{m}) = \displaystyle\prod_{r=1}^{d} W_{k_r,i_r}(m_r), \quad \forall \mathbf{i} \in \mathcal{R}^d. \end{cases}$$

are the eigenvalues and corresponding orthogonal eigenvectors of $\boldsymbol{\mathcal{S}}_{\mathbf{k}}$.

As a result of Eq. (4.3), the solution $\hat{\underline{U}}_{\mathbf{k}}$ in the frequency domain can be computed with an optimised algorithm that we give henceforth. It is based on tensorisation and the use of internal variables.

Inversion of the symbol by SVD. As for the one-dimensional case, Eq. (4.7) can be rewritten, for any frequency $\mathbf{k} \in \mathcal{N}^d$, as

$$\hat{\underline{U}}_{\mathbf{k}} = \boldsymbol{\mathcal{S}}_{\mathbf{k}}^{-1}\, \hat{\underline{F}}_{\mathbf{k}} = \sum_{\mathbf{p}} \lambda_{\mathbf{k},\mathbf{p}}^{-1}\, \underline{V}_{\mathbf{k},\mathbf{p}}\, \underline{V}_{\mathbf{k},\mathbf{p}}^{*}\, \boldsymbol{\mathcal{M}}_d\, \hat{\underline{F}}_{\mathbf{k}}, \tag{4.9}$$

where $\boldsymbol{\mathcal{M}}_d$ denotes the mass matrix in d-dimensions, and it can be rewritten as

$$\boldsymbol{\mathcal{M}}_d(\mathbf{i}, \mathbf{m}) = \prod_{r=1}^{d} \boldsymbol{\mathcal{M}}(i_r, m_r).$$

Equation (4.9) can be re-written,

$$\begin{aligned} \hat{U}_{\mathbf{k}}(\mathbf{j}) &= \sum_{\mathbf{p}} \sum_{\mathbf{r}} \lambda_{\mathbf{k},\mathbf{p}}^{-1} V_{\mathbf{k},\mathbf{p}}(\mathbf{j})\, \overline{V_{\mathbf{k},\mathbf{p}}(\mathbf{r})}\, \boldsymbol{\mathcal{M}}_d(\mathbf{r}) \hat{F}_{\mathbf{k}}(\mathbf{r}) \\ &= \sum_{\mathbf{p}} \lambda_{\mathbf{k},\mathbf{p}}^{-1} V_{\mathbf{k},\mathbf{p}}(\mathbf{j}) \sum_{\mathbf{r}} \overline{V_{\mathbf{k},\mathbf{p}}(\mathbf{r})}\, \boldsymbol{\mathcal{M}}_d(\mathbf{r}) \hat{F}_{\mathbf{k}}(\mathbf{r}). \end{aligned} \tag{4.10}$$

From Eq. (4.10), we see that the total number of operations required to compute all the components of $\hat{\underline{U}}_{\mathbf{k}}$ is $O(R^{3d})$, that is comparable to the cost of symbol inversion by standard algorithms (e.g. by Gaussian elimination). As an illustration, this inversion would require $O(R^9)$ operations in 3 dimensions, and since typical value of R are larger than 3 in our application this prevents the method to be used naively. Fortunately, we have shown in Corollary 4.3 that the eigenvalues and eigenvectors in higher dimensions can be directly derived by tensorisation from those in 1-D. This will be used to define an optimised algorithm. First, we introduce two intermediate variables, and we split Eq. (4.10) into three main operations:

- We define $\alpha_{\mathbf{k}}(\mathbf{p})$ as

$$\alpha_{\mathbf{k}}(\mathbf{p}) = \sum_{\mathbf{r}} \overline{V_{\mathbf{k},\mathbf{p}}(\mathbf{r})}\, \boldsymbol{\mathcal{M}}_d(\mathbf{r}) \hat{F}_{\mathbf{k}}(\mathbf{r}); \tag{4.11}$$

- Then, we compute the scalar coefficients $\gamma_{\mathbf{k}}(\mathbf{p})$ as

$$\gamma_{\mathbf{k}}(\mathbf{p}) \coloneqq \lambda_{\mathbf{k},\mathbf{p}}^{-1}\, \alpha_{\mathbf{k}}(\mathbf{p});$$

- Finally, the components $\hat{U}_{\mathbf{k}}(\mathbf{j})$ are retrieved as

$$\hat{U}_{\mathbf{k}}(\mathbf{j}) = \sum_{\mathbf{p}} \gamma_{\mathbf{k}}(\mathbf{p})\, V_{\mathbf{k},\mathbf{p}}(\mathbf{j}). \tag{4.12}$$

Now, we can take advantage of the properties of the eigenvalues $V_{\mathbf{k},\mathbf{p}}(\mathbf{j})$. Due to Eq.(4.3), we can reduce the two multi-dimensional sums in Eq. (4.11) and Eq. (4.12) in successions of one-dimensional sums. In order to avoid cumbersome expressions, we consider $d = 2$ henceforth. Note, however, that the extension of our analysis for $d > 2$ is straightforward. The intermediate coefficient $\alpha_{\mathbf{k}}(\mathbf{p})$ is computed, for each $\mathbf{p}$, in $O(R)$ operations by

$$\begin{aligned}
\alpha_{\mathbf{k}}(\mathbf{p}) = \alpha_{\mathbf{k}}(p_1, p_2) &\coloneqq \sum_{r_1, r_2 \in \mathcal{R}} \boldsymbol{\mathcal{M}}_d(r_1, r_2) \hat{F}_{\mathbf{k}}(r_1, r_2)\, \overline{V_{k_1,p_1}(r_1)}\, \overline{V_{k_2,p_2}(r_2)} \\
&= \sum_{r_2 \in \mathcal{R}} \overline{V_{k_2,p_2}(r_2)} \sum_{r_1 \in \mathcal{R}} \boldsymbol{\mathcal{M}}_d(r_1, r_2) \hat{F}_{\mathbf{k}}(r_1, r_2)\, \overline{V_{k_1,p_1}(r_1)} \\
&= \sum_{r_2 \in \mathcal{R}} \overline{V_{k_2,p_2}(r_2)}\, \beta_{\mathbf{k}}(p_1, r_2),
\end{aligned} \tag{4.13}$$

where $\beta_{\mathbf{k}}(\mathbf{p})$ is computed in $O(R)$ operations and is given by

$$\beta_{\mathbf{k}}(\mathbf{p}) = \beta_{\mathbf{k}}(p_1, p_2) \coloneqq \sum_{r_1 \in \mathcal{R}} \boldsymbol{\mathcal{M}}_d(r_1, p_2)\, \hat{F}_{\mathbf{k}}(r_1, p_2) \overline{V_{k_1,p_1}(r_1)}.$$

Analogously, $\hat{U}_{\mathbf{k}}(\mathbf{j})$, for a given $\mathbf{j}$, is obtained in $O(R)$ operations as follows

$$\begin{aligned}
\hat{U}_{\mathbf{k}}(\mathbf{j}) = \hat{u}_{\mathbf{k}}(j_1, j_2) &= \sum_{p_1, p_2 \in \mathcal{R}} \gamma_{\mathbf{k}}(p_1, p_2)\, V_{k_1,p_1}(j_1)\, V_{k_2,p_2}(j_2) \\
&= \sum_{p_2 \in \mathcal{R}} V_{k_2,p_2}(j_2) \sum_{p_1 \in \mathcal{R}} \gamma_{\mathbf{k}}(p_1, p_2)\, V_{k_1,p_1}(j_1) \\
&= \sum_{p_2 \in \mathcal{R}} V_{k_2,p_2}(j_2)\, \mu_{\mathbf{k}}(j_1, p_2),
\end{aligned} \tag{4.14}$$

with $\mu_{\mathbf{k}}(\mathbf{j})$ again computed in $O(R)$ operations by

$$\mu_{\mathbf{k}}(\mathbf{j}) = \mu_{\mathbf{k}}(j_1, j_2) \coloneqq \sum_{p_1 \in \mathcal{R}} \gamma_{\mathbf{k}}(p_1, j_2)\, V_{k_1,p_1}(j_1).$$

Consequently, the overall complexity of the algorithm for the symbol inversion for each frequency is $O(R^4)$. For arbitrary dimension d the complexity is $O(R^{d+1})$. Therefore, in 3-D this represents $O(R^5)$ less operations than the naive approach, that is a tremendous gain.

4.2. Neumann or Dirichlet boundary conditions. The algorithm in the d-dimensional case can be directly deduced by tensorisation also when homogeneous

Dirichlet or Neumann conditions are imposed at the boundaries. In order to perform the DFT, the source term is periodically and symmetrically extended in d directions. This leads to the evaluation of a computational domain that is potentially 2^d times larger than the original domain. However, due to the symmetry properties of the extended source term, we will be able to reduce the main computations to the first $(N+1)^d$ frequencies. The extended discrete source term $\left\{f_{\mathbf{n},\mathbf{j}}\right\}$ satisfies, for all $r \in \{1,\cdots,d\}$,

$$\begin{cases} f_{\mathbf{n}+\mathbf{n}_r,\mathbf{j}} = \pm f_{\mathbf{n},\mathbf{j}+\mathbf{j}_r}, & j_r \neq 0, \quad \mathbf{n}_r = \mathbf{e}_r(2N-1-n_r),\, \mathbf{j}_r = \mathbf{e}_r(R-j_r), \\ f_{\mathbf{n}+\mathbf{n}_r,\mathbf{j}} = \pm f_{\mathbf{n},\mathbf{j}}, & j_r = 0, \quad \mathbf{n}_r = \mathbf{e}_r(2N-n_r), \end{cases} \tag{4.15}$$

where $\mathbf{e}_r$ is the $r-$th vector of the canonical basis of $\mathbb{R}^d$ and (n_r, j_r) is such that

$$\mathbf{n}+\mathbf{n}_r \in \{0,\cdots,2N-1\}^d, \quad \mathbf{j}+\mathbf{j}_r \in \{0,\cdots R-1\}^d,$$

and where the even extension corresponds to Neumann BCs, while the odd extension is associated with Dirichlet BCs, as before.

LEMMA 4.4. *The DFT of the extended sequence* $\left\{f_{\mathbf{n},\mathbf{j}}\right\}$ *satisfies,* $\forall r \in \{1,\cdots,d\}$,

$$\begin{cases} \hat{f}_{\mathbf{k}+\mathbf{k}_r,\mathbf{j}} = \pm \hat{f}_{\mathbf{k},\mathbf{j}+\mathbf{j}_r}\, e^{\frac{-i\pi k}{N}}, & \text{if } \; j_r \neq 0, \quad \mathbf{k}_r = \mathbf{e}_r(2N-k_r),\, \mathbf{j}_r = \mathbf{e}_r(R-j_r), \\ \hat{f}_{\mathbf{k}+\mathbf{k}_r,\mathbf{j}} = \pm \hat{f}_{\mathbf{k},\mathbf{j}}, & \text{if } \; j_r = 0, \quad \mathbf{k}_r = \mathbf{e}_r(2N-k_r), \end{cases}$$

with (k_r, j_r) *such that*

$$\mathbf{k}+\mathbf{k}_r \in \{0,\cdots,2N-1\}^d, \quad \mathbf{j}+\mathbf{j}_r \in \{0,\cdots R-1\}^d$$

and with the usual convention for the plus and minus signs.

Therefore, given a direction $i \in \{1,2,..,d\}$, the value of the DFT coefficients for the last $N-1$ coefficients in that direction are directly retrieved from the first N coefficients, and the relationship depends on the frequency and the Gauss-Lobatto point taken into account.

Eventually, due to Lemma 4.4 and Proposition 3.3, the solution $\hat{u}_{\mathbf{k},\mathbf{j}}$ inherits the same properties of $\hat{f}_{\mathbf{k},\mathbf{j}}$. Therefore, the optimised algorithm to solve (4.2), when homogeneous Neumann or Dirichlet conditions are considered, is

1. Perform a DFT of the discrete source term for each order $\mathbf{j}$ fixed in $\mathcal{R}$

$$\hat{f}_{\mathbf{k},\mathbf{j}} = \sum_{\mathbf{n}\,\in\,\{0,..,(2N-1)\}^d} f_{\mathbf{n},\mathbf{j}}\, e^{\frac{-i\pi\mathbf{n}\cdot\mathbf{k}}{N}}, \;\; \forall \mathbf{k} \in (\mathcal{N}\cup\{N\})^d,$$

   using Eq. (4.15) for evaluating $f_{\mathbf{n},\mathbf{j}}$ when $\mathbf{n} \notin \mathcal{N}^d$;
2. Solve for each frequency

$$\boldsymbol{\mathcal{S}}_{\mathbf{k}}\, \underline{\hat{U}}_{\mathbf{k}} = \underline{\hat{F}}_{\mathbf{k}}, \;\; \forall \mathbf{k} \in (\mathcal{N}\cup\{N\})^d;$$

3. Perform an inverse DFT for each order $\mathbf{j}$ fixed in $\mathcal{R}$

$$u_{\mathbf{n},\mathbf{j}} = \frac{1}{(2N)^d} \sum_{\mathbf{n}\,\in\,\{0,..,(2N-1)\}^d} \hat{u}_{\mathbf{k},\mathbf{j}}\, e^{\frac{i\pi\mathbf{n}\cdot\mathbf{k}}{N}}, \;\; \forall \mathbf{n} \in (\mathcal{N}\cup\{N\})^d,$$

Figure 4 Convergence of the two-dimensional scheme w.r.t. the space step h, for different values of order R. Left: Relative $L^2(\Omega)$-error. Right: Relative $H^1(\Omega)$-error.

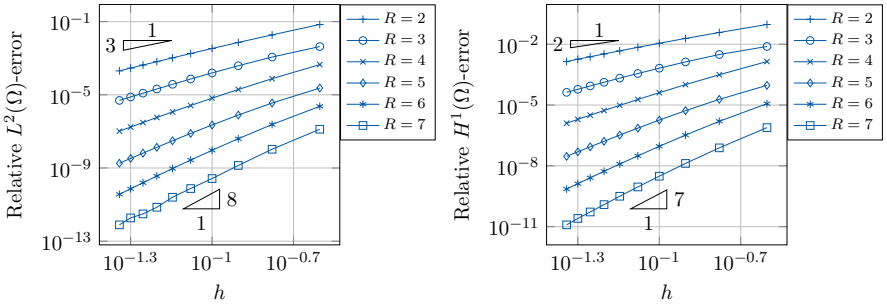

where, thanks to Lemma 4.4,

$$\begin{cases} \hat{u}_{\mathbf{k}+\mathbf{k}_r,\mathbf{j}} = \pm \hat{u}_{\mathbf{k},\mathbf{j}+\mathbf{j}_r}\, e^{\frac{-i\pi k}{N}}, & \text{if } \; j_r \neq 0, \quad \mathbf{k}_r = \mathbf{e}_r(2N - k_r),\, \mathbf{j}_r = \mathbf{e}_r(R - j_r), \\ \hat{u}_{\mathbf{k}+\mathbf{k}_r,\mathbf{j}} = \pm \hat{u}_{\mathbf{k},\mathbf{j}}, & \text{if } \; j_r = 0, \quad \mathbf{k}_r = \mathbf{e}_r(2N - k_r), \end{cases}$$

with the usual convention for signs, and with (k_r, j_r) such that

$$\mathbf{k} + \mathbf{k}_r \in \{0, \cdots, 2N-1\}^d, \quad \mathbf{j} + \mathbf{j}_r \in \{0, \cdots R-1\}^d.$$

It is possible to do an efficient implementation of Steps 1 and 3 that never requires the storage and the pre-computation of the odd or even extensions. On the contrary, Eq. (4.15) is used on-the-flight, for an improved performance in terms of storage and memory access time.

5. Numerical Results, complexity and parallelisation.

5.1. Convergence analysis. In order to demonstrate that the HO-DFT method preserves the order of convergence of the underlying SEM discretisation, the method is tested against an exact solution of Problem (2.1) with $\rho = 0$ and homogeneous Dirichlet Boundary conditions, that reads

$$u(\underline{x}) = \prod_{i=1}^{d} (1 - x_i)^3\, x_i^3\, \cos(k\, x_i), \quad \forall \underline{x} \in \Omega = [0,1]^d, \; d = 2, 3,$$

with $k = 10$. Figures 4 and 5 show the convergence error between the exact solution and the output of the HO-SEM algorithm in relative $L^2(\Omega)$ and $H^1(\Omega)$ norm w.r.t. the space step h in two and three dimensions, for different values of order R. The convergence rate of the error in $L^2(\Omega)$ and $H^1(\Omega)$-norm corresponds to the chosen order R.

5.2. Complexity of the algorithm. As it has been stated in the previous sections, this algorithm is remarkably efficient in multiple dimensions, for multiple reasons. Firstly, an efficient algorithm – in $O(R^{d+1})$ operations – has been deduced for Step 2 of each algorithm, that relies on the tensorisation properties of the underlying finite elements. Secondly, Steps 1 and 3 can be performed by FFT. Since d-dimensional FFT corresponds to a 1-D FFT having the size of the product of the dimensions, its complexity is $d(\log N)N^d$ (if the domain is divided into the same number of elements N for each direction). Consequently, the implementation of FFT

Figure 5 Convergence of the three-dimensional scheme w.r.t. the space step h, for different values of order R. Left: Relative $L^2(\Omega)$-error. Right: Relative $H^1(\Omega)$-error.

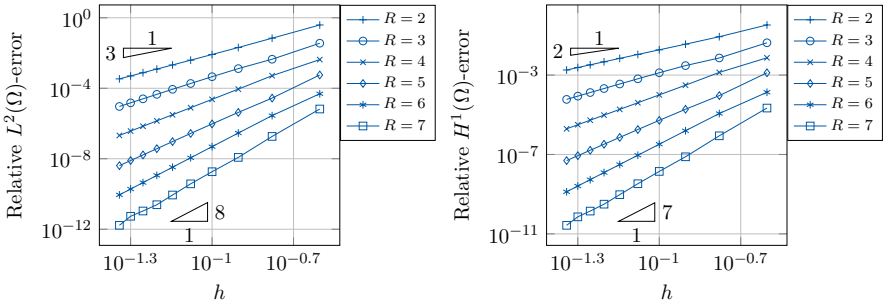

Figure 6 Computational cost of the three-dimensional scheme. Comparison for different numbers of threads.

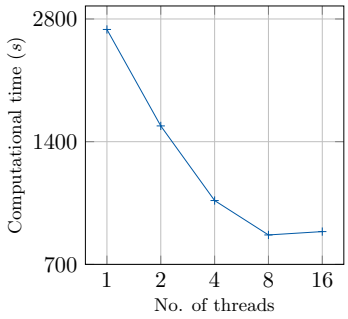

causes a further, sensible reduction of the computational cost.

We emphasise that this method is not limited to the solution of the Poisson-like problem with periodic boundary conditions. In fact, we have shown that, in case of Dirichlet or Neumann BCs, it is possible to employ HO-DFT after extending symmetrically or anti-symmetrically the computational domain – i.e. the number of frequencies considered – in each dimension. However, thanks to symmetry properties of the sequence considered and Fourier Transform, most operations only involve the first $N + 1$ spatial frequencies (in each direction), and therefore the computational overcost of the algorithm is reduced. Besides, Steps 1 and 3 are disjoint for each order, whereas the operations involved in the inversion of the symbol (Step 2) are disjoint for each frequency. Therefore, the algorithm is extremely well-adapted to parallelisation. In particular, Steps 1 and 3 can be run in parallel for each order, whereas Step 2 can be performed in parallel for each frequency. Figure 6 depicts a performance analysis when multi-threading is used. Note that the performance is optimal for 8 threads and worsens for 16 threads on a 12-cores workstation (cores at 2.7 GHz and 64 GB of RAM at 1867 MHz). Figure 7 shows the computational cost of the sequential solution of the problem with homogeneous Dirichlet Boundary conditions in 3-D on a 4-cores workstation (cores at 3.1 GHz and 16 GB of RAM at 1867 MHz). The computational time is in accordance with the expected complexity with respect to the number of elements N and the order R. Finally, note that the memory storage is minimised and, apart from the solution vector, only the eigenvector and eigenvalues of the matrices $\boldsymbol{\mathcal{N}}_k$ – that correspond to 1-D symbols – must be stored for each scalar frequency k.

Figure 7 Computational cost of the three-dimensional scheme. Left: comparison for different values of elements. Right: comparison for different values of order R.

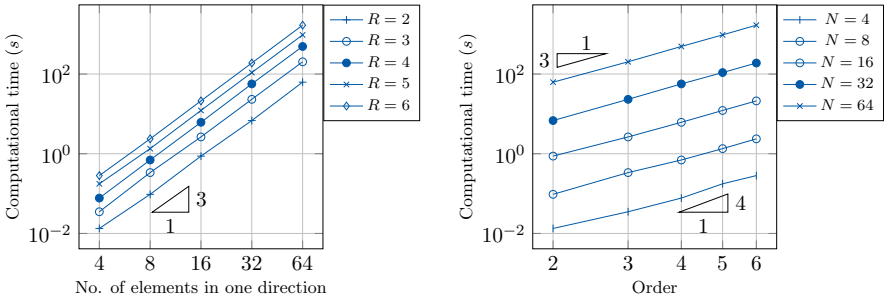

REFERENCES

[1] Mark Ainsworth. Discrete dispersion relation for hp-version finite element approximation at high wave number. *SIAM Journal on Numerical Analysis*, 42(2):553–575, 2004.

[2] Mark Ainsworth and Patrick Coggins. A uniformly stable family of mixed hp-finite elements with continuous pressures for incompressible flow. *IMA journal of numerical analysis*, 22(2):307–327, 2002.

[3] Faisal Amlani and Oscar P. Bruno. An fc-based spectral solver for elastodynamic problems in general three-dimensional domains. *Journal of Computational Physics*, 307:333 – 354, 2016.

[4] Steffen Börm, Lars Grasedyck, and Wolfgang Hackbusch. Introduction to hierarchical matrices with applications. *Engineering analysis with boundary elements*, 27(5):405–422, 2003.

[5] Franco Brezzi and Richard S Falk. Stability of higher-order hood–taylor methods. *SIAM Journal on Numerical Analysis*, 28(3):581–590, 1991.

[6] Franco Brezzi and Michel Fortin. *Mixed and hybrid finite element methods*, volume 15. Springer Science & Business Media, 2012.

[7] G. Cohen. *Higher-Order Numerical Methods for Transient Wave Equations*. Scientific Computation. Springer Berlin Heidelberg, 2001.

[8] Gary Cohen. *Higher-Order Numerical Methods for Transient Wave Equations*. Scientific computation. Springer, 2002.

[9] Gary Cohen and Sandrine Fauqueux. Mixed spectral finite elements for the linear elasticity system in unbounded domains. *SIAM Journal on Scientific Computing*, 26(3):864–884, 2005.

[10] Jean-Luc Guermond, Peter Minev, and Jie Shen. An overview of projection methods for incompressible flows. *Computer methods in applied mechanics and engineering*, 195(44-47):6011–6045, 2006.

[11] B. Gustafsson. *Fundamentals of Scientific Computing*. Texts in Computational Science and Engineering. Springer Berlin Heidelberg, 2011.

[12] Arieh Iserles. *A first course in the numerical analysis of differential equations*. Number 44. Cambridge university press, 2009.

[13] Dimitri Komatitsch and Jean-Pierre Vilotte. The spectral element method: an efficient tool to simulate the seismic response of 2d and 3d geological structures. *Bulletin of the seismological society of America*, 88(2):368–392, 1998.

[14] Mark Lyon and Oscar P. Bruno. High-order unconditionally stable fc-ad solvers for general smooth domains ii. elliptic, parabolic and hyperbolic pdes; theoretical considerations. *Journal of Computational Physics*, 229(9):3358 – 3381, 2010.

[15] Yvon Maday and Anthony T Patera. Spectral element methods for the incompressible navier-stokes equations. In *State-of-the-art surveys on computational mechanics (A90-47176 21-64). New York, American Society of Mechanical Engineers. Research supported by DARPA.*, pages 71–143, 1989.

[16] Alfio Quarteroni, Riccardo Sacco, and Fausto Saleri. *Numerical mathematics*, volume 37. Springer Science & Business Media, 2010.

[17] Charles Van Loan. *Computational frameworks for the fast Fourier transform*, volume 10. Siam, 1992.